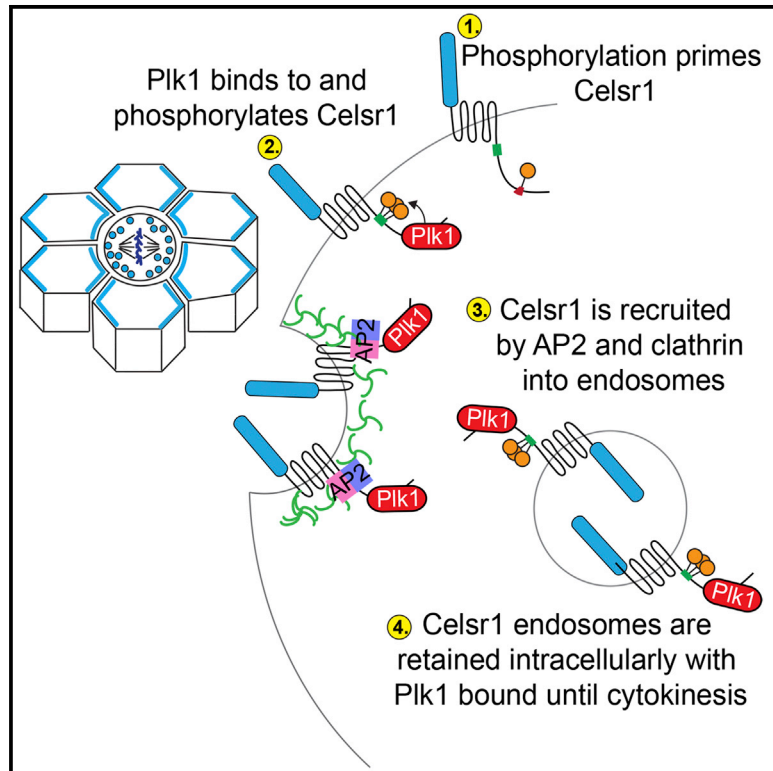


# Developmental Cell

## Mitotic Control of Planar Cell Polarity by Polo-like Kinase 1

### Graphical Abstract



### Authors

Rezma Shrestha, Katherine A. Little, ..., David H. Perlman, Danelle Devenport

### Correspondence

danelle@princeton.edu

### In Brief

In polarized epithelial cells, planar cell polarity (PCP) proteins are internalized during mitosis and then redistributed with cell-cycle progression. Shrestha et al. now show that the mitotic regulator Polo-like kinase 1 (Plk1) coordinates this process via phosphorylation of the PCP protein Celsr1, which promotes Celsr1 endocytosis during mitosis.

### Highlights

- Plk1 localizes to mitotic endosomes and phosphorylates Celsr1's endocytic motif
- Plk1-dependent phosphorylation is necessary for Celsr1 mitotic endocytosis
- Celsr1 recruits Plk1 via a PBD-binding motif required for internalization
- Phosphomimetic mutations can uncouple Celsr1 internalization from mitosis



# Mitotic Control of Planar Cell Polarity by Polo-like Kinase 1

Rezma Shrestha,<sup>1</sup> Katherine A. Little,<sup>1</sup> Joel V. Tamayo,<sup>1</sup> Wenyang Li,<sup>1</sup> David H. Perlman,<sup>2</sup> and Danelle Devenport<sup>1,\*</sup>

<sup>1</sup>Department of Molecular Biology, Princeton University, Princeton, NJ 08544, USA

<sup>2</sup>Department of Chemistry, Princeton University, Princeton, NJ 08544, USA

\*Correspondence: [danelle@princeton.edu](mailto:danelle@princeton.edu)

<http://dx.doi.org/10.1016/j.devcel.2015.03.024>

## SUMMARY

During cell division, polarized epithelial cells employ mechanisms to preserve cell polarity and tissue integrity. In dividing cells of the mammalian skin, planar cell polarity (PCP) is maintained through the bulk internalization, equal segregation, and polarized recycling of cortical PCP proteins. The dramatic redistribution of PCP proteins coincides precisely with cell-cycle progression, but the mechanisms coordinating PCP and mitosis are unknown. Here we identify Plk1 as a master regulator of PCP dynamics during mitosis. Plk1 interacts with core PCP component Celsr1 via a conserved polo-box domain (PBD)-binding motif, localizes to mitotic endosomes, and directly phosphorylates Celsr1. Plk1-dependent phosphorylation activates the endocytic motif specifically during mitosis, allowing bulk recruitment of Celsr1 into endosomes. Inhibiting Plk1 activity blocks PCP internalization and perturbs PCP asymmetry. Mimicking dileucine motif phosphorylation is sufficient to drive Celsr1 internalization during interphase. Thus, Plk1-mediated phosphorylation of Celsr1 ensures that PCP redistribution is precisely coordinated with mitotic entry.

## INTRODUCTION

Cell polarity is the fundamental unit of epithelial architecture, characterized by the asymmetric localization of cortical polarity proteins (Goodrich and Strutt, 2011; Roignot et al., 2013). When epithelial cells divide, they employ mechanisms to ensure these cortical asymmetries are preserved or tissues risk disorganization and loss of epithelial integrity. To preserve apical-basal polarity, the mitotic spindle aligns parallel to the substratum such that both daughter cells inherit cortical polarity proteins equally (Fernández-Miñán et al., 2007; Hao et al., 2010; Jaffe et al., 2008; Reinsch and Karsenti, 1994). We previously identified a mechanism whereby rapidly dividing basal cells of the mammalian skin preserve planar cell polarity (PCP) via mitotic internalization of cortical PCP components (Devenport et al., 2011). Mitotic internalization erases and restores PCP with every cell division and must therefore be precisely coordinated with cell-cycle progression, but the mechanisms regulating this process are not known.

PCP is defined by the collective alignment of cell polarity along the epithelial plane. The process is controlled by a set of conserved “core” PCP proteins, including Celsr (Flamingo/Fmi in *Drosophila*), Frizzled (Fz), Vangl (VanGogh/Vang), Dishevelled (Dvl), and Prickle (Pk), which orient diverse structures including *Drosophila* wing hairs and mammalian hair follicles (Goodrich and Strutt, 2011; Simons and Mlodzik, 2008; Vladar et al., 2009). PCP proteins localize asymmetrically within the cell, with Fz and Dvl positioned opposite Vangl and Pk (Axelrod, 2001; Bastock et al., 2003; Strutt, 2001; Strutt and Strutt, 2009; Tree et al., 2002). These complexes associate intercellularly via homotypic bridges formed by the seven-pass transmembrane cadherin Celsr/Fmi (Chen et al., 2008; Lawrence et al., 2004; Struhl et al., 2012; Usui et al., 1999). Local disruptions to PCP propagate non-autonomously to neighboring cells (Simons and Mlodzik, 2008; Taylor et al., 1998; Vinson and Adler, 1987), highlighting the need for PCP maintenance during tissue growth and regeneration.

In mammalian skin, PCP controls the coordinated alignment of hair follicles (HFs), which is maintained despite lifelong proliferation and regeneration (Devenport and Fuchs, 2008; Devenport et al., 2011; Guo et al., 2004; Ravi et al., 2009). HF alignment relies on PCP function in interfollicular basal cells, highly proliferative progenitors that give rise to the outer stratified skin layers and HFs (Devenport and Fuchs, 2008). When basal cells divide, asymmetrically localized PCP components become rapidly and selectively internalized into endosomes, segregated equally into daughter cells, and recycled to the plasma membrane where asymmetry is restored (Devenport et al., 2011). Forced cortical retention of PCP proteins during division causes tissue-wide defects in HF alignment, demonstrating the necessity of mitotic endocytosis to preserve global PCP.

To elucidate the mechanisms controlling PCP during mitosis, we undertook a proteomic approach to identify mitosis-specific posttranslational modifications (PTMs) and interacting partners of Celsr1. We demonstrate that the key mitotic kinase, Plk1, is a Celsr1-interacting protein essential for mitotic internalization. Celsr1 contains a conserved PBD-binding motif required for internalization and Plk1 association. Plk1 directly phosphorylates conserved serine/threonine (S/T) residues near Celsr1's dileucine endocytic motif, which allows the AP2 adaptor complex and clathrin to recruit Celsr1 into endosomes. Inhibition of Plk1 diminishes Celsr1 phosphorylation and blocks mitotic internalization, leading to the disruption of Celsr1 asymmetry *ex vivo*. Finally, mimicking dileucine motif phosphorylation uncouples Celsr1 internalization from mitosis and bypasses the

requirement for Plk1 function. Together, these results explain how the dramatic rearrangement of PCP proteins is precisely coordinated with the onset of mitosis.

## RESULTS

### Mitosis-Specific Phosphorylation of Celsr1 Endocytic Motif Coordinates Internalization with Mitotic Progression

To understand the mechanisms targeting PCP proteins for bulk internalization in mitosis, we focused on Celsr1 because it acts upstream in the process, being both necessary and sufficient to recruit Vangl2 and Fz6 to mitotic endosomes (Devenport and Fuchs, 2008; Devenport et al., 2011). Mitotic internalization of Celsr1 requires a juxtamembrane dileucine motif (Devenport et al., 2011), a common sorting motif that is recognized by the AP2 adaptor complex to initiate clathrin-mediated endocytosis (Traub and Bonifacino, 2013). Celsr1 internalizes at the onset of prophase in vivo as shown by the complete redistribution of membrane-localized Celsr1 into bright intracellular puncta upon first detection of the mitotic marker, pH3 (Figures 1A and 1B). Exogenous Celsr1 $\Delta$ N-GFP, lacking the N-terminal extracellular domain, internalizes in cultured keratinocytes with the same temporal dynamics observed for full-length Celsr1 in vivo (Figure 1C) and thus provides a useful tool to address how Celsr1's endocytic motif is recognized exclusively during mitosis.

To identify mitosis-specific interacting partners and PTMs on Celsr1, we performed a comparative mass spectrometry (MS)-based analysis of Celsr1 in dividing and non-dividing cells. Mouse keratinocytes stably expressing Celsr1 $\Delta$ N-GFP were grown either asynchronously or synchronized in mitosis, and Celsr1 $\Delta$ N-GFP coimmunoprecipitates were analyzed by MS/MS. Coimmunoprecipitates from non-GFP wild-type cells served as controls for non-specific binding. We identified over 300 Celsr1-associated proteins that were enriched in mitotic samples (Figure 1D; Tables S1 and S2). Among the most abundant of these was the mitotic kinase Plk1. Plk1 is a S/T kinase essential for mitotic entry and progression (Barr et al., 2004; Elia et al., 2003a, 2003b) and thus is a likely candidate to provide cell-cycle control of PCP internalization.

We also identified 20 S/T phosphorylation sites on Celsr1's cytoplasmic tail, three of which were clustered around its dileucine endocytic motif (Figure 1E; Tables S3 and S4). By comparing peak intensities of extracted ion chromatographs, we found that all three sites were enriched in mitotically synchronized samples compared with their asynchronous counterparts (S2714, 2.2-fold; T2750, 2.9-fold; T2752, 1.3-fold) (Figures 1F and S1). We hypothesized that phosphorylation near the dileucine endocytic motif (designated as dileucine motif phosphorylation hereafter) might determine the specificity of PCP internalization during mitosis.

### Plk1 Colocalizes with Internalized Celsr1 during Mitosis

Plk1 was a likely candidate to control mitotic PCP internalization because of its central role in promoting early mitotic events, but the protein was not known to localize to the plasma membrane or to endosomes. To determine the localization of Plk1 in dividing keratinocytes, we coexpressed Plk1-YFP with Celsr1 $\Delta$ N-Flag.

In addition to the previously described localization of Plk1 at centrosomes and kinetochores (Barr et al., 2004; Park et al., 2010), Plk1-YFP adopted punctate localization in the cytoplasm that overlapped with internalized Celsr1 $\Delta$ N-Flag (Figure 2A). Colocalization between Plk1 and Celsr1 was first observed during early prophase and persisted through metaphase, anaphase, and telophase (Figure 2A). At cytokinesis, Plk1 localized exclusively to the cytokinesis furrow, whereas Celsr1 reestablished cortical membrane localization (Figure 2A). To confirm these dynamics in living cells, we performed time-lapse microscopy on keratinocytes coexpressing Plk1-YFP and Celsr1 $\Delta$ N-mCherry. Plk1 and Celsr1 overlap was first detected in prophase and persisted until midzone formation in early cytokinesis when Plk1 was displaced from Celsr1 endosomes (Figure 2B; Movies S1 and S2). Endogenous Plk1 also localized to Celsr1 puncta, as detected by Plk1 antibody staining (Figure 2C). To assess whether Plk1 associated with Celsr1 at the cell surface at newly forming endosomes, total internal reflection fluorescence (TIRF) microscopy was performed on cells coexpressing Plk1-YFP and Celsr1 $\Delta$ N-Flag. Plk1-YFP and Celsr1 $\Delta$ N-Flag overlapped at surface puncta at early prophase (Figure 2D), indicating that Plk1 associates with Celsr1 from the earliest stages of endosome formation. These findings are both consistent with previous Plk1 localization studies and demonstrate that, upon entry into mitosis, Plk1 is recruited to sites of Celsr1 internalization.

### Celsr1 Contains a PBD-Binding Motif Required for Plk1 Association and Mitotic Internalization

Plk1 is targeted to specific subcellular locations by binding to proteins harboring a PBD-binding motif with the minimal and invariant consensus sequence S-P-T-P (maximal binding follows the consensus  $\Phi$ /P- $\Phi$ -T/Q/H/M-S-pT/pS-P/X; Elia et al., 2003a, 2003b). It is thought that threonine phosphorylation of PBD-binding motifs primes the site for Plk1 binding (Lee et al., 2008; Neef et al., 2007). Close examination of Celsr1's cytoplasmic domain revealed the presence of a well-conserved PBD-binding motif (PAHSTP) (Figures 3A and 3C). Moreover, our MS-based proteomic analyses also revealed that Celsr1's STP site is threonine-phosphorylated (pT2864), suggesting Plk1 could interact directly with Celsr1 (Table S3). To determine whether Celsr1's PBD-binding motif is required for its internalization, we first generated truncations of the Celsr1 cytoplasmic tail in the context of an E-Cadherin-Celsr1-GFP hybrid construct (termed E-Celsr1CT-GFP henceforth), which encodes a protein chimera fusing the C terminus of Celsr1 to the extracellular and transmembrane domains of E-Cadherin (Figure 3A). E-Celsr1CT-WT-GFP displays mitotic internalization into the same endocytic compartment as full-length Celsr1, indicating that the regulatory sequences contained in Celsr1's 319-amino acid cytosolic tail are sufficient to drive mitotic internalization (Devenport et al., 2011). Deletion of the C-terminal 180 amino acids removed the PBD-binding motif and blocked Celsr1 internalization (Figures 3B and 3C). However, inclusion of the PBD-binding motif by reducing the deleted region to 160 amino acids had no effect, demonstrating that nearly half of the cytoplasmic tail is dispensable for mitotic endocytosis. The degree of internalization in the E-Celsr1CT mutants was quantified by calculating the colocalization coefficients between each mutant and wild-type Celsr1 $\Delta$ N-Flag, which was cotransfected as an internal control. Alanine substitution of

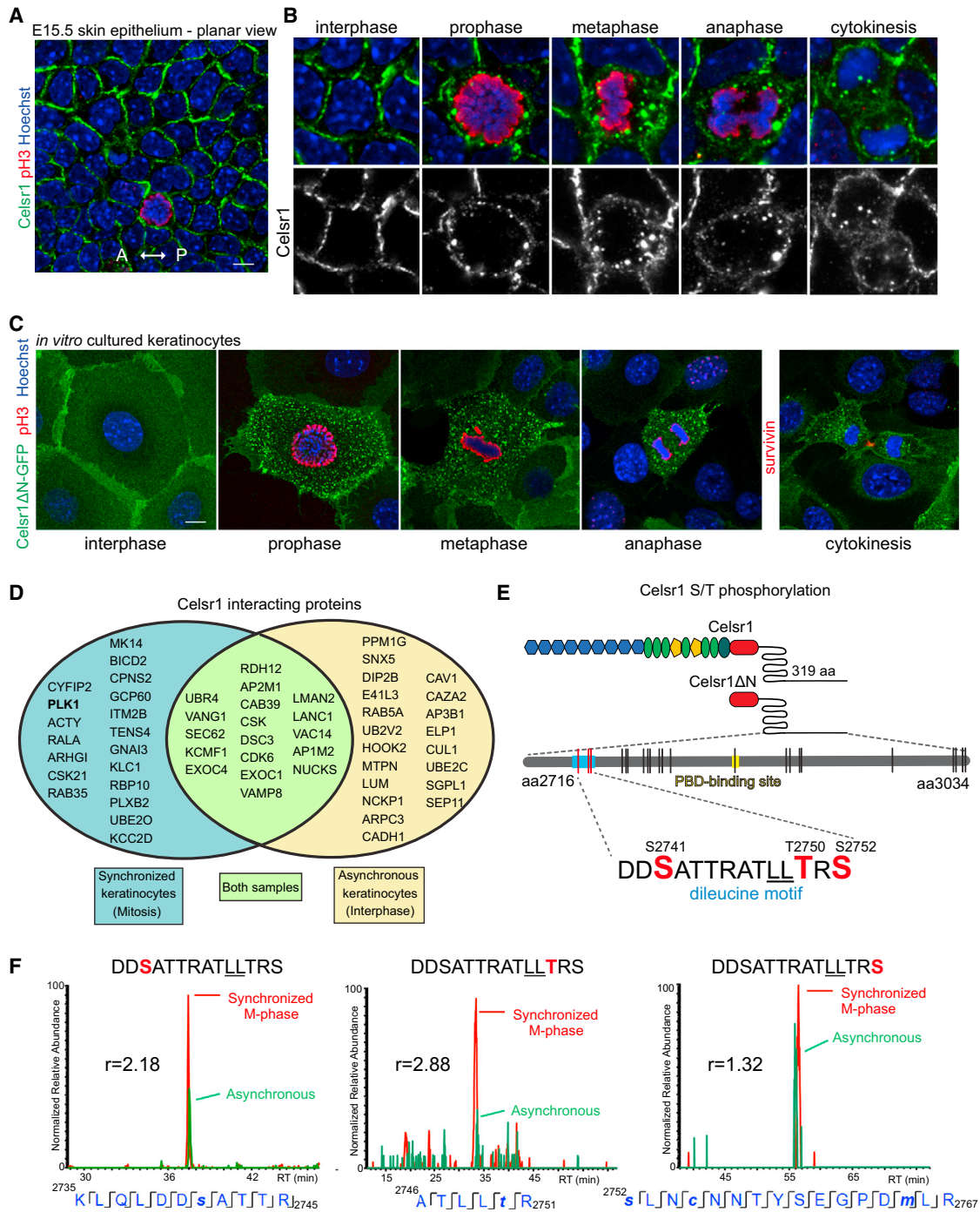


**Figure 1. Mitosis-Specific Celsr1 Interactors and Phosphorylation Sites Identified by Mass Spectrometry**

(A) Single confocal section through basal layer of E15.5 whole-mount backskins labeled with Celsr1 (green), phospho-histone H3, a marker of mitotic progression (pH3, red), and Hoechst (blue). Anterior is to the left. Note the anterior-posterior enrichment of Celsr1 at cell-cell contacts.

(B) Representative images of Celsr1 localization in basal cells at indicated cell-cycle stages, labeled as in (A).

(C) Cultured keratinocytes stably expressing a truncated form of Celsr1, Celsr1ΔN-GFP (green), labeled with pH3 or survivin (red), and Hoechst (blue). Representative examples of the indicated mitotic stages are shown. Note that upon mitotic entry, Celsr1 is internalized in bulk from the cell surface. Celsr1-containing endosomes are held within the cytoplasm throughout metaphase and anaphase and recycled to the surface upon cytokinesis.

Scale bars, 10 μm.

(D) Venn diagram shows selected Celsr1-associated proteins enriched in synchronized (blue), asynchronous (yellow), or both populations of keratinocytes (green) as identified by coimmunoprecipitation and MS. Selected proteins (including Plk1) displayed the highest number of spectral counts compared with controls, excluding metabolic enzymes and “housekeeping” proteins. See [Tables S1](#) and [S2](#) for complete list.

(legend continued on next page)

the threonine alone (T2864A) also reduced internalization of both the E-Celsr1CT-GFP chimera and Celsr1 $\Delta$ N-GFP, demonstrating a functional requirement for the PBD-binding motif (Figure 3B). This result was initially unexpected because previous deletion mapping in the context of full-length Celsr1 narrowed the sequences required for internalization to a smaller region of the cytoplasmic tail that lacked the PBD-binding domain (Figure S2; Devenport et al., 2011). Closer inspection of this deletion mutant, Celsr1 $\Delta$ 2754–3034-GFP, revealed a partial defect in mitotic internalization that was rescued by the addition of excess full-length Celsr1-Flag (Figure S2). Rescue is not observed in Celsr1 variants lacking the N-terminal extracellular domain (Devenport et al., 2011), suggesting the redundancy is mediated by N-terminal cis-interactions. We conclude that Celsr1's PBD-binding domain is important for internalization, but its function can be bypassed when wild-type full-length Celsr1 is present (Figure S2).

To assess whether the PBD-binding motif is required for the Celsr1-Plk1 interaction, we tested the ability of the Celsr1 cytoplasmic tail containing the T2864A mutation to coimmunoprecipitate Plk1-GFP. Immunoprecipitation of wild-type E-Celsr1CT-Flag efficiently coprecipitated Plk1-GFP from transfected keratinocyte lysates, but the T2864A mutant showed substantially reduced efficiency (Figure 3D). Furthermore, immunoprecipitation of Plk1-GFP efficiently coprecipitated wild-type E-Celsr1CT-Flag, but not the T2864A mutant (Figure 3D). These findings suggest that a PBD-dependent interaction between Celsr1 and Plk1 is an important step in Celsr1 mitotic internalization.

### Plk1 Phosphorylates the Celsr1 Cytoplasmic Domain In Vitro

The PBD-dependent interaction between Celsr1 and Plk1 suggested that Plk1 might promote mitotic endocytosis by directly phosphorylating Celsr1's dileucine sorting motif. To test this possibility, we performed an in vitro kinase assay between bacterially expressed GST-Celsr1CT and His-tagged Plk1. Plk1 demonstrated specific and robust kinase activity toward the 319-amino acid cytoplasmic domain of Celsr1 (Figure 3E). Analysis of in vitro phosphorylated Celsr1 peptides by MS/MS identified 14 S/T residues phosphorylated by Plk1, five of which were located near the dileucine motif including S2741, T2750, and S2752, which we found to be phosphorylated at higher levels during mitosis (Figures 3E and 1F; Table S5). Four of the 14 Plk1 phosphosites conform to the classical Plk1 substrate consensus sequence D(E)XpS/T (Nakajima et al., 2003), but most do not, including T2750 and S2752, consistent with a broad consensus for Plk1 substrates (Kettenbach et al., 2011; Santamaria et al., 2011). Together, these results suggest a model in which Plk1 triggers Celsr1 internalization by binding to its PBD-binding motif, phosphorylating residues adjacent to its dileucine sorting signal, and activating its clathrin-

dependent endocytosis in a mitosis-specific manner. If this model is correct, the earliest steps of Celsr1 endocytosis should rely on Plk1.

### Inhibition of Plk1 Blocks Mitotic Internalization

To test whether Plk1 is required for mitotic endocytosis, keratinocytes stably expressing Celsr1 $\Delta$ N-GFP were treated with BI2536, a potent and selective inhibitor of Plk1 (Lénárt et al., 2007; Steegmaier et al., 2007). Whereas control cells treated with DMSO displayed normal mitotic endocytosis of Celsr1 $\Delta$ N-GFP, treatment with BI2536 led to prometaphase arrest and completely blocked Celsr1 $\Delta$ N-GFP internalization (Figures 4A and 4B). To rule out the possibility that the failure to internalize Celsr1 was due to mitotic arrest, we compared Plk1-inhibited cells with keratinocytes treated with an inhibitor targeting Aurora A and B (VX-680). Treatment with Aurora A/B inhibitor led to mitotic arrest in prometaphase, but internalization of Celsr1 was not affected (Figures 4A and 4B). Additionally, transferrin internalized normally in BI2536-arrested cells demonstrating a specific requirement for Plk1 in Celsr1 mitotic internalization (Figure 4C).

We then performed time-lapse TIRF microscopy of Celsr1 recruitment into clathrin-coated vesicles (CCVs) to determine which step of endocytosis requires Plk1. In control cells treated with DMSO, bright Celsr1 $\Delta$ N-GFP puncta formed at the surface of mitotic cells that colocalized with  $\mu$ 2-mRFP (marking the AP2 adaptor complex) and DsRed-Clathrin (Figures 4D and 4E). In Plk1-inhibited cells,  $\mu$ 2-mRFP and DsRed-Clathrin localized to punctate structures that internalized with normal kinetics, but Celsr1 $\Delta$ N-GFP never coalesced into surface puncta, remaining smoothly localized to the plasma membrane (Figures 4D and 4E; Movie S3). These results demonstrate that Plk1 acts at the earliest stages of endocytosis to induce clustering and recruitment of Celsr1 cargo into AP2-CCVs. This function is selective for Celsr1-containing cargo, as AP2-CCVs appear to form normally at the cell surface upon Plk1 inhibition, whereas Celsr1 fails to be recruited into them.

### Plk1 Function Is Required in the Skin Epithelium for Celsr1 Mitotic Internalization and Asymmetric Localization

We next examined the role of Plk1 in the developing skin epithelium. Mouse embryonic skin explants (E14.5) were grown ex vivo in the presence of DMSO or mitotic inhibitors for 4 hr. Consistent with our in vitro findings, explants treated with Aurora A/B or Plk1 inhibitors displayed an accumulation of basal cells arrested in prometaphase, but only inhibition of Plk1 blocked Celsr1 internalization (Figures 5A–5D). The cortical retention of Celsr1 in Plk1-inhibited mitotic cells allowed us to address whether the cell shape changes that accompany mitosis have any effect on the maintenance of Celsr1 asymmetry. Indeed, whereas Celsr1 localized with bipolar asymmetry to anterior and posterior borders of basal

(E) Schematic of Celsr1 and Celsr1 $\Delta$ N protein domain structure, with the C-terminal cytosolic domain expanded below. Black lines represent phosphorylated S/T residues in Celsr1 $\Delta$ N-GFP identified by MS. See Tables S3 and S4 for complete list. The dileucine motif (turquoise, sequence shown below) is surrounded by six S/T residues, three of which (S2741, T2750, and S2752, red lines) were differentially phosphorylated in mitosis.

(F) Extracted ion chromatograms of phosphopeptides containing S2741, T2750, and S2752 from synchronous and asynchronous samples are shown overlaid following normalization by the intensities of their non-phosphorylated analogs present in each LC/MS run. R value = normalized ratio of phosphopeptide abundance in synchronous versus asynchronous cells. See Table S4 and Figure S1 for MS1 and MS/MS spectra.

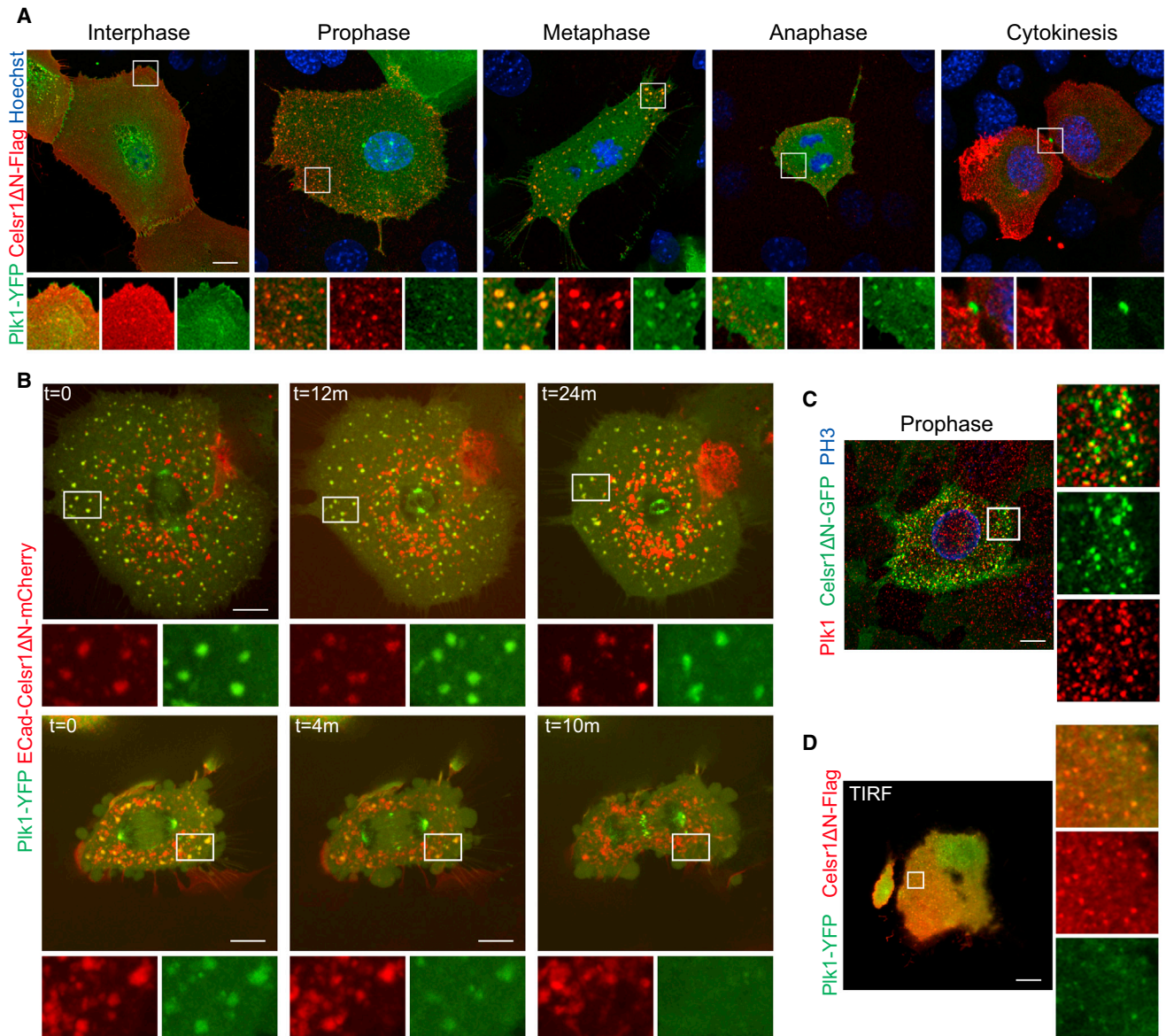


**Figure 2. PIK1 Localizes to Celsr1-Containing Endosomes during Mitosis**

(A) Keratinocytes were cotransfected with plasmids encoding PIK1-YFP (green) and Celsr1 $\Delta$ N-Flag (red). Nuclei were labeled with Hoechst (blue). Representative images at the indicated stages of mitosis are shown. Insets show 2 $\times$  magnified single and merged channels. Celsr1 and PIK1 colocalize at endosomes during prophase, metaphase, and anaphase/telophase. By cytokinesis, the two proteins no longer colocalize.

(B) Time-lapse images from PIK1-YFP (green) and ECad-Celsr1 $\Delta$ N-mCherry (red) coexpressing keratinocyte. Insets show magnified single channels. Top: prophase to metaphase. Bottom: telophase to cytokinesis. Note that PIK1 dissociates from Celsr1-containing endosomes during cytokinesis. See also [Movies S1](#) and [S2](#).

(C) Endogenous PIK1 colocalizes with Celsr1 $\Delta$ N-GFP in mitosis. Anti-PIK1 polyclonal antibody is shown in red and Celsr1 $\Delta$ N-GFP in green.

(D) Mitotic keratinocyte expressing PIK1-YFP (green) and Celsr1 $\Delta$ N-Flag (red) in early prophase imaged by TIRF microscopy. The two fluorescent proteins colocalize at surface puncta at the earliest stages of mitosis.

Scale bars, 10  $\mu$ m

cells in interphase, mitotically arrested cells with a rounded geometry often lost their polarity and displayed unipolar and non-polar Celsr1 distributions ([Figure 5C](#)). To quantify this phenotype, Celsr1 pixel intensities were plotted relative to their polar coordinates. Whereas the majority of Celsr1 pixels in interphase cells clustered around their anterior-posterior axes, Celsr1 was more randomly distributed in PIK1-inhibited mitotic cells ([Figure 5E](#)).

To assess whether mitotically arrested cells influenced the polarity of their interphase neighbors, we measured Celsr1 polarity ne-matics of interphase cells in DMSO and BI2536-treated explants. In contrast to the non-autonomous polarity defects caused by transgenic expression of Celsr1<sup>LLtoAA</sup> ([Devenport et al., 2011](#)), PIK1 inhibition did not cause a significant alteration in Celsr1 interphase polarity ([Figure 5F](#)). Thus, while cortically retained Celsr1

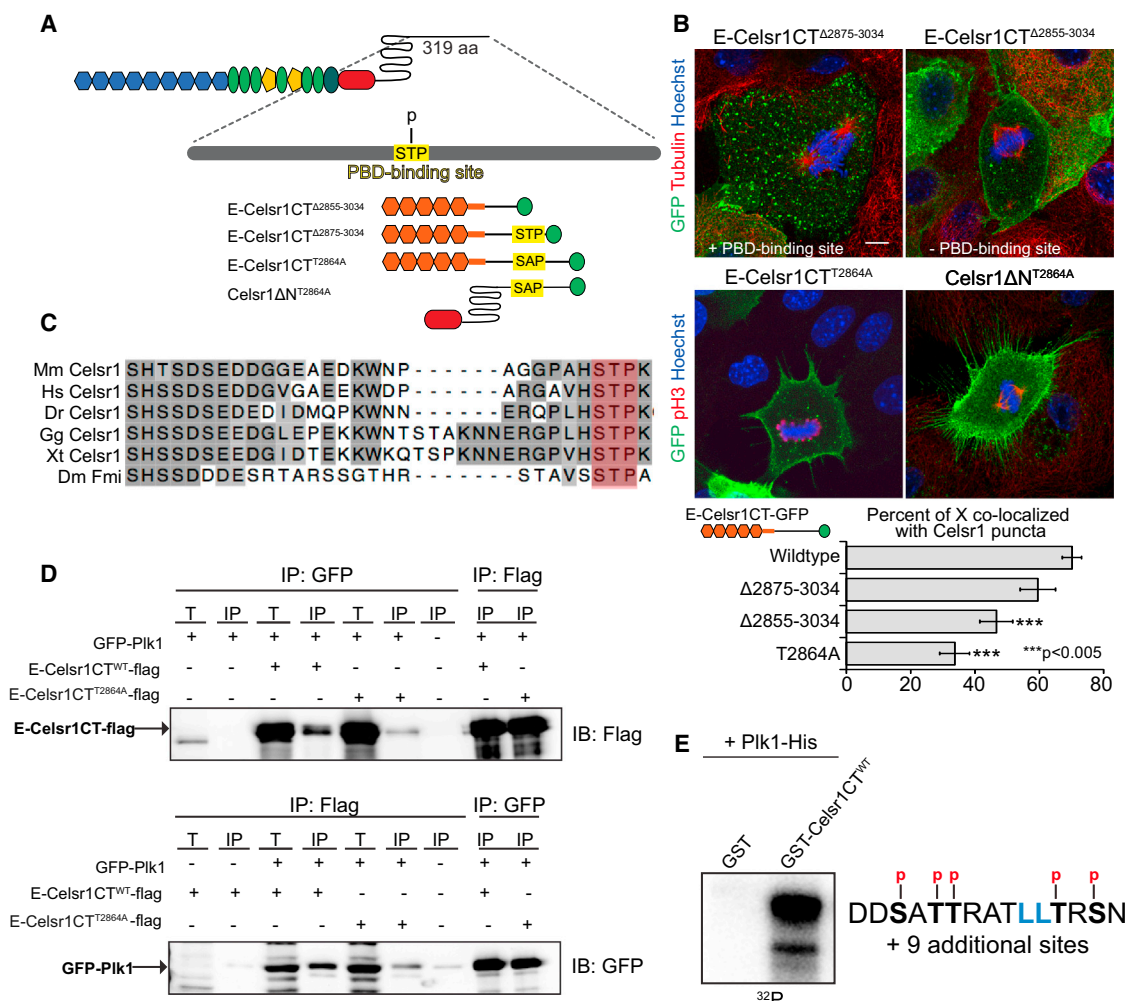


**Figure 3. Plk1 Interacts with Celsr1 via a Conserved Polo-Box Domain (PBD)-Binding Motif and Directly Phosphorylates Celsr1**

(A) Schematic of Celsr1 domain structure with the PBD-binding motif (consensus S-p-T-P) highlighted in yellow. Mutations were generated in GFP-tagged, chimeric proteins between E-Cadherin (extracellular and transmembrane domains, orange) and the cytoplasmic domain of Celsr1, as diagrammed below. E-Celsr1CT<sup>Δ2855-3034</sup> lacks the PBD and 180 C-terminal amino acids. E-Celsr1CT<sup>Δ2875-3034</sup> retains the PBD but lacks the C-terminal 160 amino acids. E-Celsr1CT<sup>T2864A</sup> and Celsr1ΔNT<sup>T2864A</sup> substitute alanine for the phosphorylated threonine in the PBD domain.

(B) Phenotypic analysis of PBD mutants as indicated in Figure 3A. Note that deletion of the PBD or alanine substitutions within the PBD impair Celsr1 endocytosis during mitosis. The mean percent colocalization between the E-Celsr1CT mutants and wild-type Celsr1 (co-transfected Celsr1ΔN-flag) during mitosis was calculated as M1 coefficients. n = 8–14 mitotic cells for each mutant (unpaired t test, error bars denote ± SEM).

(C) Alignment of amino acids 2,838 to 2,866 of the cytosolic domain of mouse Celsr1. The PBD is highlighted in pink and is highly conserved among vertebrates and in *Drosophila*.

(D) Coimmunoprecipitation of Plk1-GFP and E-Celsr1CT. Keratinocytes were transfected with expression vectors encoding Plk1-GFP and either wild-type or PBD mutant E-Celsr1CT-Flag. Reciprocal immunoprecipitations were performed from cell lysates as indicated. Coimmunoprecipitates were separated by SDS-PAGE and western blots were performed with the antibodies indicated. Note the reduced interaction between Plk1-GFP and E-Celsr1CT when the PBD is mutant (T2864A).

(E) Plk1 phosphorylates Celsr1. Kinase assay between purified Plk1 and GST alone or GST-Celsr1CT is indicated. The representative autoradiograph of incorporated  $\gamma$ -<sup>32</sup>P-ATP is shown. Plk1 phosphorylation sites on the Celsr1 cytoplasmic tail were identified by MS. Plk1 phosphorylated 5 S/T residues surrounding Celsr1's endocytic motif plus nine additional sites. See also Table S5.

Scale bars, 10  $\mu$ m

lost polarity in mitosis, this was insufficient to produce non-autonomous polarity defects, at least over the short timescales studied here. It may be that cells must progress through cytokinesis for polarity defects to be propagated to neighboring cells. Nevertheless, the loss of Celsr1 asymmetry in Plk1-inhibited mitotic cells suggests that PCP asymmetry is particularly vulnerable during mitosis.

### Mutations that Prevent Dileucine Motif Phosphorylation Impair Mitotic Internalization

To investigate the importance of S/T phosphorylation on mitotic endocytosis, we performed site-directed mutagenesis on the six conserved S/T residues surrounding Celsr1's dileucine motif (Figure 6A). Regrettably, we had previously reported that these six residues were dispensable for Celsr1 internalization, but

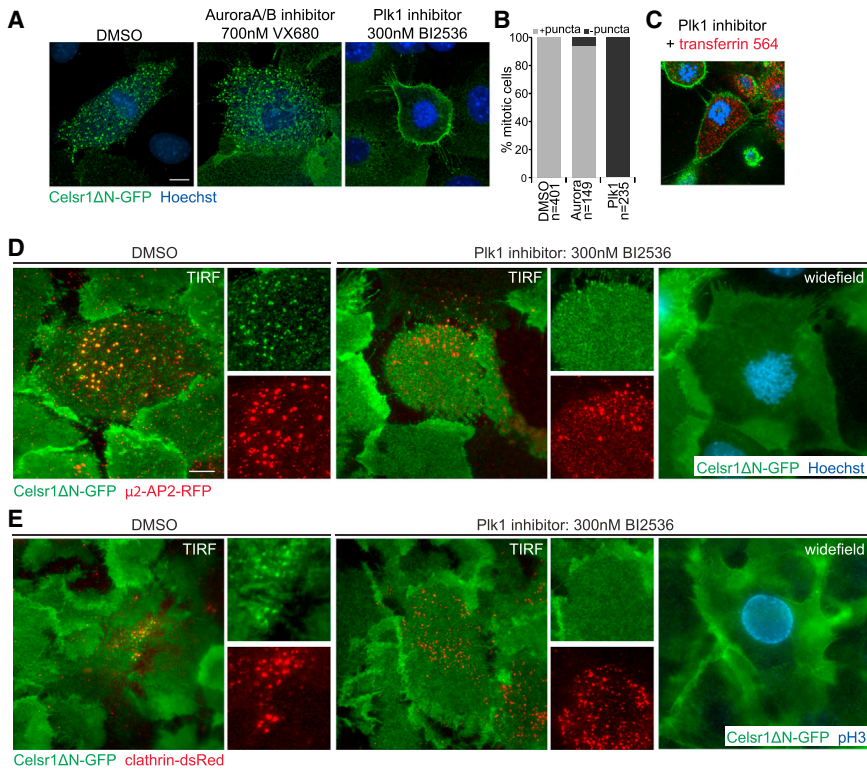


**Figure 4. Plk1 Is Essential for Mitotic Internalization**

(A) Keratinocytes stably expressing Celsr1ΔN-GFP were treated for 8 hr with mitotic kinase inhibitors or DMSO as indicated. Representative images of inhibited cells are shown. Both Aurora A/B and Plk1 inhibitors arrest cells in prometaphase. Whereas Celsr1 internalization proceeds normally upon treatment with VX-680, internalization is blocked upon Plk1 inhibition.

(B) Quantification of the percentage of mitotic keratinocytes containing Celsr1 endosomes treated with DMSO or inhibitor of kinase indicated. Plk1 inhibition blocks internalization completely.

(C) Plk1 inhibition does not block transferrin internalization (red), which accumulates normally in BI2536-arrested cells.

(D and E) Analysis of clathrin-coated pit formation upon Plk1 inhibition.

(D) Celsr1ΔN-GFP (green) keratinocytes coexpressing μ2-mRFP (red) were imaged by TIRF microscopy. Separate channels are shown to the right of the merged images. Control cells in mitosis (DMSO) display characteristic bright Celsr1-puncta at the cell surface that colocalize with μ2-mRFP. In Plk1-inhibited mitotic cells (300 nM BI2536, 3 hr), Celsr1ΔN-GFP fails to coalesce into punctate structures at the cell surface and remains uniformly localized similar to the surrounding interphase cells. Note that μ2-mRFP still forms cell surface puncta in the presence of

BI2536. Widefield image of the same BI2536-treated cell is shown to the right confirming the imaged cell was in mitosis.

(E) TIRF images of control and Plk1 inhibited (300 nM BI2536, 3 hr) keratinocytes in mitosis coexpressing Celsr1ΔN-GFP (green) and clathrin-dsRed (red). Whereas clathrin puncta form normally at the surface of Plk1-inhibited cells, Celsr1 is not recruited to them. Widefield image of the same BI2536-treated cell labeled with pH3 (blue) confirms the cell was in mitosis. See also [Movie S3](#).

Scale bars, 10 μm.

revisiting the original mutant construct revealed an error in the sequence ([Devenport et al., 2011](#), correction). To reexamine the function of Celsr1 S/T phosphorylation, alanine substitutions were introduced singly or in combination into the E-Celsr1CT-GFP hybrid construct, and keratinocytes were cotransfected with wild-type Celsr1ΔN-Flag as an internal control for quantification. Mutation of all six S/T residues (STTTTS → 6A) completely blocked internalization in mitosis, closely mimicking the dileucine mutant defect ([Figures 6B and 6C](#)). To further map essential phosphosites, we separately mutated the four proximal (STTT → 4A) and two distal (TS → 2A) S/T residues flanking the dileucine sequence. Whereas E-Celsr1CT-4A-GFP internalized similar to wild-type, internalization of E-Celsr1CT-2A-GFP was strongly inhibited, though not to the full extent of the 6A mutant ([Figures 6B and 6C](#)). Single alanine substitutions for T2750 or S2752 alone produced only minimal effects on internalization ([Figure 6C](#)), suggesting functional redundancy between the phosphorylated sites. These results were confirmed in the context of Celsr1ΔN-GFP ([Figure S3](#)), confirming that E-Celsr1CT chimeras provide a useful tool to examine Celsr1 endocytic regulation.

### Phosphorylation of Celsr1's Endocytic Sorting Motif Is Mitosis Specific and Plk1 Dependent

Next, we generated a phospho-specific antibody against p-T2750 to investigate the spatial and temporal distribution of phosphory-

lated Celsr1. Purified polyclonal antibodies raised against peptides containing p-T2750 recognized only the phosphorylated version of the peptide in dot blots and do not immunolabel the Celsr1 T2750A cytoplasmic tail mutant, demonstrating the phospho-specificity of the antibody ([Figure S4](#)). Next we performed immunostaining of Celsr1ΔN-GFP expressing keratinocytes with anti-Celsr1-pT2750. The antibody specifically labeled the internalized pool of Celsr1 in mitotic cells, beginning at prophase and persisting through telophase ([Figures 6D and S4](#)). By contrast, anti-Celsr1-pT2750 did not detect membrane-localized Celsr1 during interphase or in mitotic cells treated with the Plk1 inhibitor ([Figures 6D and S4](#)). This localization pattern was corroborated in vivo, where Celsr1-pT2750 colocalized with a subset of Celsr1-containing endosomes in mitotic cells, but not with cortical, asymmetrically localized Celsr1 in interphase ([Figure 6E](#)). The spatial and temporal localization pattern of Celsr1-pT2750 closely mirrored that of endosomal Plk1 ([Figure 2](#)), suggesting that Plk1 may be responsible for T2750 phosphorylation. Indeed, inhibiting Plk1 eliminated Celsr1-pT2750 labeling in mitosis ([Figure 6D](#)).

To further assess whether Celsr1 phosphorylation is Plk1 dependent, we analyzed Celsr1ΔN-GFP phosphopeptides in the presence of Plk1 inhibitor by MS and found a 10-fold reduction in the pS2741 peptide abundance compared with DMSO treated controls ([Figure S5 and Table S4](#)). Although peptides containing T2750 and S2752 were unfortunately not recovered

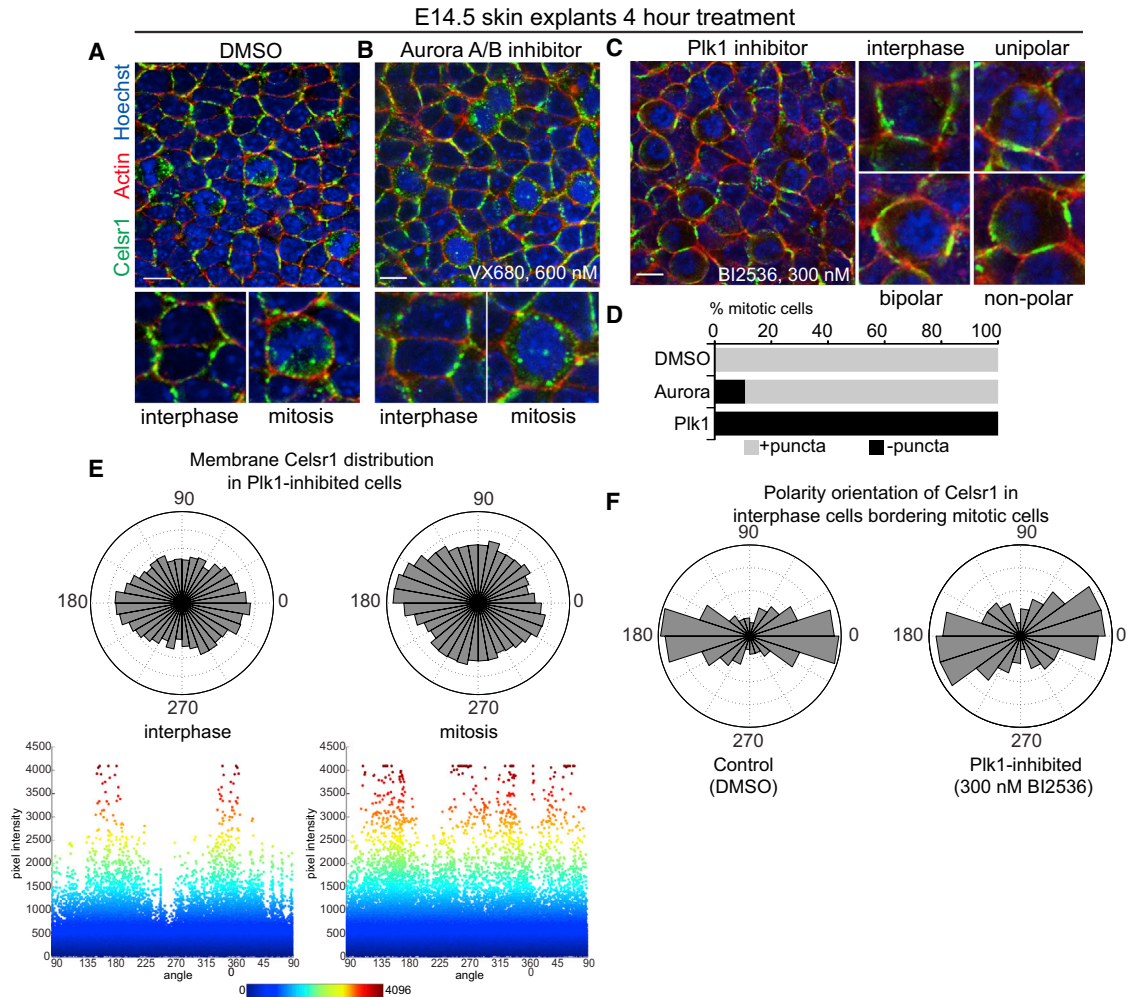


### Figure 5. Ex Vivo Inhibition of Plk1 Inhibits PCP Mitotic Internalization and Impairs Celsr1 Asymmetry

(A–C) Backskin explants from E14.5 embryos were cultured and treated with (A) DMSO, (B) Aurora A/B inhibitor VX680, or (C) Plk1 inhibitor BI2536 for 4 hr. Representative images of interphase and mitotic cells are shown. Many cells arrest in mitosis upon both Plk1 and Aurora A/B inhibition. Note that while VX680-treated mitotic cells internalize Celsr1, the mitotic cells treated with BI2536 display aberrant Celsr1 localization, here classified broadly as bipolar, unipolar, or non-polar. This is different from the anterior-posterior localization of Celsr1 seen in interphase cells.

(D) Percentage of mitotic cells containing Celsr1 endosomes in explants treated with DMSO ( $n = 54$ ), Plk1 inhibitor ( $n = 388$ ), or Aurora inhibitor ( $n = 269$ ).

(E) Roseplots (top) and scatterplots (bottom) of Celsr1 pixel intensities and their corresponding angles in interphase ( $n = 86$ ) versus mitotic ( $n = 76$ ) cells in Plk1-inhibited explants. Note that mitotic cells display a more uniform distribution of Celsr1 around the cell perimeter than interphase cells.

(F) Angular distribution of Celsr1 polarity in interphase cells bordering mitotic cells in DMSO ( $n = 183$ ) and BI2536-treated explants ( $n = 218$ ). The anterior-posterior axis is horizontal and anterior is to the left.

Scale bars, 10  $\mu\text{m}$ .

in the Plk1-inhibited MS run, we found a 2.5-fold reduction in the SpTP-containing peptide (T2864), suggesting Plk1 may “self-prime” Celsr1’s PBD-binding motif (Figure S4). In sum, our data demonstrate that dileucine motif phosphorylation is mitosis specific, Plk1 dependent, and essential for Celsr1 mitotic internalization.

### Phosphomimetic Mutations Uncouple Celsr1 Internalization from Mitosis and Bypass the Requirement for Plk1

To determine whether phosphorylation of the endocytic motif is sufficient for Celsr1 internalization, we generated phosphomimetic versions of Celsr1 $\Delta\text{N}$ -GFP and examined their localization

dynamics in interphase. Although just two alanine mutations (T2750A and S2752A) were sufficient to inhibit internalization in mitosis, replacing these two sites with glutamate (TS $\rightarrow$ 2E) failed to induce Celsr1 endocytosis during interphase (Figure 7A). Mutation of all six S/T residues surrounding the dileucine motif (6E), however, caused a dramatic redistribution of interphase Celsr1. Whereas wild-type Celsr1 $\Delta\text{N}$ -GFP displayed smooth plasma membrane localization in interphase, the Celsr1 $\Delta\text{N}$ -6E-GFP mutant displayed a striking punctate distribution with a concomitant loss of diffuse membrane localization (Figure 7A). A subset of Celsr1 $\Delta\text{N}$ -6E-GFP interphase puncta colocalized with Rab5-dsRed, a marker of early endosomes (Figure 7B). To confirm Celsr1 $\Delta\text{N}$ -6E-GFP puncta were indeed endosomes,

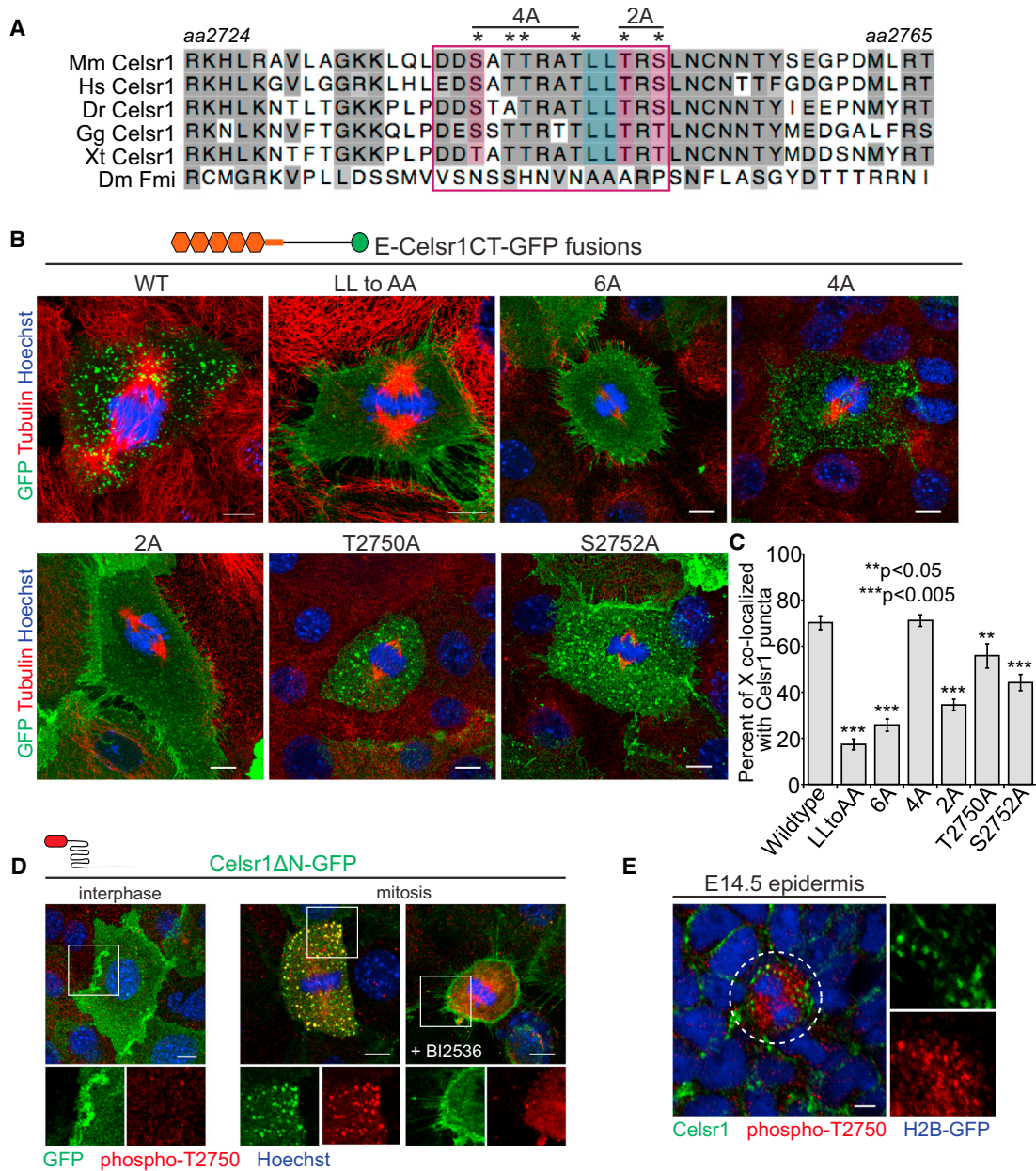


**Figure 6. Celsr1 Phosphorylation during Mitosis Is Required for Its Mitotic Internalization**

(A) Alignment of the cytosolic domain (R2724-T2765) of mouse Celsr1 and other indicated species. The dileucine and surrounding S/T residues are highly conserved across vertebrates. Asterisks denote residues targeted for mutagenesis. The dileucine is highlighted in blue, and phosphorylated S/T residues are shaded in pink.

(B) Mutagenesis of S/T residues. Keratinocytes were transfected with E-Celsr1CT constructs as indicated. Spindles are labeled with  $\beta$ -tubulin (red) and nuclei labeled by Hoechst (blue). Mutations targeting S/T residues surrounding the dileucine motif are indicated above representative images. E-Celsr1CT-6A contains alanine mutations corresponding to amino acids S2741, T2743, T2744, T2747, T2750, and S2752 in full-length Celsr1. E-Celsr1CT-4A is mutated to alanine at positions corresponding to S2741, T2743, T2744, and T2747. E-Celsr1CT-2A contains alanine mutations at positions corresponding to T2750 and S2752.

(C) Quantification of colocalization (M1 coefficients averaged across 16–25 mitotic cells for each mutant) between S/T mutants and cotransfected wild-type Celsr1 $\Delta$ N-flag during mitosis, as described in Figure 3. Unpaired t test, error bars denote  $\pm$  SEM. Note that internalization is most strongly inhibited in the 6A and 2A mutants, as well as the T2864A mutant (shown in Figure 3B).

(D) Localization of phospho-T2750 Celsr1. A Celsr1 phospho-specific polyclonal antibody was raised against peptides containing phospho-T2750. Keratinocytes stably expressing Celsr1 $\Delta$ N-GFP were immunolabeled with purified anti-phospho-T2750 (red) and Hoechst (blue). Note that the phospho-specific antibody labels Celsr1 endosomes in mitosis, but not cortical Celsr1 during interphase or in PLK1-inhibited mitotic cells.

(E) Whole-mount backskin from K14-H2BGFP transgenic E14.5 embryo labeled with anti-phospho-T2750 (red) and Celsr1 (green) antibodies. A single confocal plane through the basal layer is shown.

Scale bars, 10  $\mu$ m.

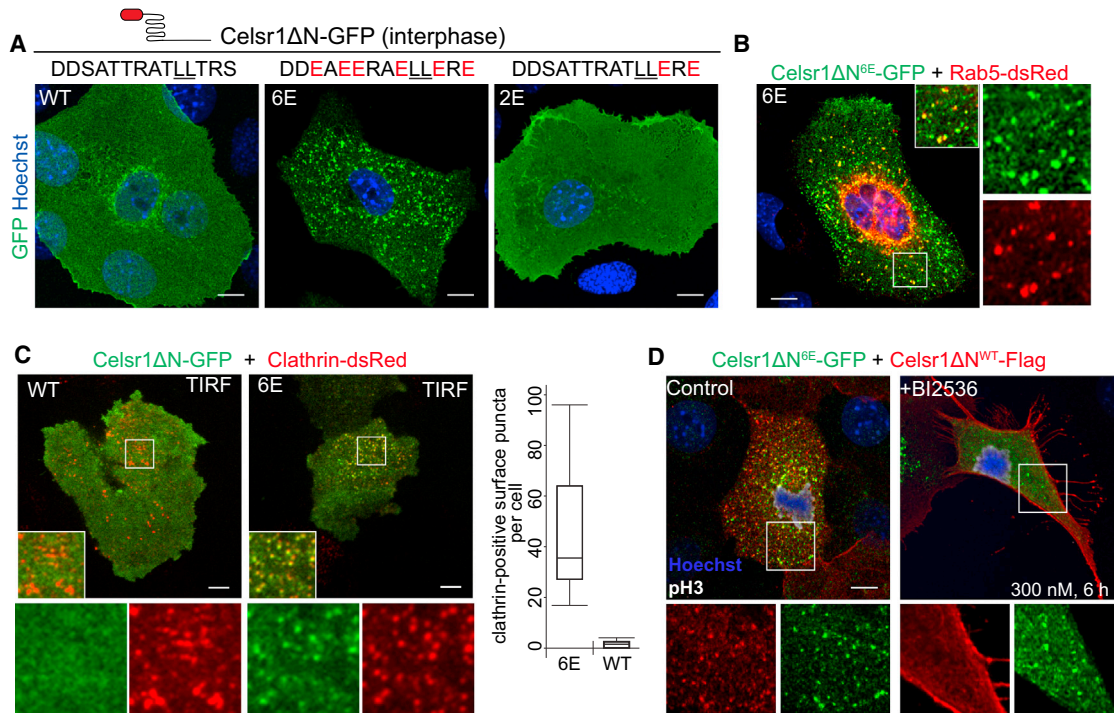


**Figure 7. Phosphomimicking Mutations Uncouple Celsr1 Internalization from Mitosis**

Serine or threonine residues surrounding the dileucine motif were mutated to glutamic acid in Celsr1ΔN-GFP (green) as indicated.

(A) Interphase keratinocytes transfected with the indicated phosphomimicking mutations. Nuclei were labeled by Hoechst (blue). Whereas both wild-type Celsr1 and the 2E mutant display smooth plasma membrane localization during interphase, the 6E mutant accumulates in punctate structures.

(B) Confocal image of interphase keratinocyte coexpressing the early endosome marker Rab5-dsRed (red) and Celsr1ΔN<sup>6E</sup>-GFP (green) showing colocalization during interphase.

(C) Interphase keratinocytes coexpressing clathrin-dsRed (red) and Celsr1ΔN<sup>WT</sup>-GFP or Celsr1ΔN<sup>6E</sup>-GFP (green) were imaged by TIRF microscopy. Interphase Celsr1ΔN<sup>6E</sup>-GFP puncta colocalize with clathrin-dsRed at the cell surface. Quantification of clathrin-positive puncta seen by TIRF on the cell surface of interphase cells expressing wild-type Celsr1 (n = 8) and Celsr1ΔN<sup>6E</sup>-GFP (n = 10). See also [Movie S4](#).

(D) Localization of Celsr1ΔN<sup>6E</sup>-GFP in mitosis. Keratinocytes cotransfected with Celsr1ΔN<sup>6E</sup>-GFP (green) and Celsr1ΔN<sup>WT</sup>-flag (red) in the presence (300 nM BI2536, 6 hr) or absence (control) of Plk1 inhibitor. Whereas Celsr1ΔN<sup>WT</sup>-flag mitotic internalization is Plk1 dependent, Celsr1ΔN<sup>6E</sup>-GFP remains punctate even in the presence of BI2536.

Scale bars, 10 μm.

we performed time-lapse TIRF imaging of clathrin-dsRed/Celsr1ΔN-6E-GFP coexpressing cells and observed accumulation of GFP puncta that colocalized with clathrin at the surface, remarkably similar to wild-type Celsr1ΔN during mitosis ([Figure 7C](#); [Movies S3](#) and [S4](#)). These results strongly suggest that phosphorylation of Celsr1's endocytic sorting signal restricts the timing of its internalization to mitosis.

Finally, to determine whether the requirement for Plk1 in Celsr1 internalization can be bypassed by mimicking dileucine motif phosphorylation, we examined the mitotic localization of Celsr1ΔN-6E-GFP in cells treated with BI2536. Cotransfection of Celsr1ΔN-WT-Flag served as an internal control and upon Plk1 inhibition, was retained at the membrane. In contrast, the Celsr1ΔN-6E-GFP mutant did not require Plk1 for its internalization and remained punctate even in BI2536-treated cells ([Figure 7D](#)). These results indicate that the major function of Plk1 in regulating mitotic internalization is the phosphorylation of Celsr1's endocytic sorting motif. Together these data support a model where Plk1-dependent phosphorylation of Celsr1's dileucine motif activates the endocytic sorting signal to induce mitosis-specific internalization.

## DISCUSSION

Mitosis is perhaps the most vulnerable time in a cell's life. During division, the cell dismantles much of its interphase architecture to segregate the chromosomes and organelles into two daughter cells. This is potentially detrimental for cells assembled into complex epithelial patterns, whose integrity must simultaneously be maintained while allowing for tissue growth and homeostasis. Epithelial disorganization is invariably associated with carcinomas, and loss of polarity is strongly associated with metastatic behavior ([Martin-Belmonte and Perez-Moreno, 2012](#)). Our previous study identified selective mitotic endocytosis of PCP proteins as a mechanism to preserve PCP in a rapidly dividing epithelium. We proposed that mitotic endocytosis enables asymmetrically distributed PCP proteins to be equally segregated to daughter cells irrespective of the plane of division while preventing dividing cells from sending or receiving PCP cues as they change shape and rearrange ([Devenport et al., 2011](#)). Consistent with this notion, we find that when mitotic endocytosis is blocked via Plk1 inhibition, cortical Celsr1 often loses bipolar asymmetry, suggesting

PCP localization may be particularly sensitive to changes in cell shape.

To ensure that PCP is not dismantled at inappropriate times, we hypothesized that bulk endocytosis of PCP proteins should be carefully coordinated with mitotic progression. Here we demonstrate that the process is controlled directly by the mitotic machinery, through Plk1-mediated phosphorylation of residues near Celsr1's dileucine sorting motif. Our data indicate that during interphase, the dileucine motif is inactive and unable to be recognized by the AP2 adaptor complex. Upon Plk1 activation during the G2/M transition, Plk1 binds to Celsr1 via its PBD-binding motif and phosphorylates the endocytic motif, activating the site for AP2/clathrin recognition and bulk internalization. Priming of the PBD-binding motif by threonine-phosphorylation may add another layer of mitotic specificity to Celsr1 endocytosis, as PBD-binding domains are phosphorylated by Cdk1 or by Plk1 itself, events that occur strictly in mitosis (Lee et al., 2008). By directly activating Celsr1's endocytic motif, Plk1 ensures that bulk PCP internalization is timed precisely with mitotic entry.

The conservation of serines and threonines surrounding the dileucine motif suggests that cell-cycle-regulated endocytosis is likely a common mechanism for Celsr1 regulation, at least across vertebrates. The *Drosophila* homolog, Fmi, has not been reported to undergo mitosis-specific internalization, and consistently, none of the critical endocytic sorting residues are conserved in Fmi. The PBD-binding domain, on the other hand, is conserved in *Drosophila*, suggesting Fmi might interact with Plk1 for another function during mitosis.

PCP-containing endosomes are retained intracellularly until cytokinesis, suggesting their recycling may also be under tight cell-cycle control. Consistent with this notion, we find that inhibiting Plk1 during prophase leads to premature recycling of internalized endosomes at metaphase (data not shown), suggesting an additional role for Plk1 in endosome retention. Interestingly, Plk1 remains colocalized with Celsr1 endosomes until the onset of cytokinesis, suggesting Plk1 dissociation from mitotic endosomes may be a prerequisite for endocytic recycling. We predict cell-cycle-regulated phosphatases may also be required to deactivate the dileucine sorting motif and reset Celsr1 for interphase (Wurzenberger and Gerlich, 2011).

Only a handful of mitotic kinases including Cdk1, Aurora A/B, and Plk1 regulate multiple events required for cells to commit to, enter, and progress through mitosis (Nigg, 2001). Plk1 is known to phosphorylate hundreds of proteins required for centrosome maturation, spindle assembly, and kinetochore attachment (Elia et al., 2003a, 2003b; Santamaria et al., 2011). We can now add PCP and endocytosis to the list of Plk1-regulated processes. Proteomic analyses of Plk1 substrates list endocytic components as Plk1 targets (Lowery et al., 2007; Oppermann et al., 2012), suggesting other endocytic events could also be regulated by Plk1. Our study demonstrates that Plk1 localizes to endocytic vesicles, where it is positioned to regulate a range of intracellular trafficking proteins.

Our study also provides a proteomic analysis of Celsr1-associated proteins and PTMs. Prior to this, few proteins were known to physically associate with Celsr1 and no functionally important Celsr1 PTMs had been characterized. Our data show that at least three Celsr1 PTMs have a dramatic effect

on Celsr1 localization, and provide a list of 17 other sites that may provide additional regulation. Moreover, our catalog of Celsr1-associated proteins provides a resource for future studies focusing on Celsr1 interactions in other systems. This study helps illuminate how cells coordinate the spatial dynamics of cell polarity with the temporal progression of mitosis. Furthermore, our demonstration that polarity is regulated directly by the mitotic machinery may help to explain why in cancer, loss of polarity and uncontrolled proliferation are so closely intertwined.

## EXPERIMENTAL PROCEDURES

### Animals

Mice were housed in an AAALAC-accredited facility in accordance with the Guide for the Care and Use of Laboratory Animals. All procedures involving animals were approved by Princeton University's Institutional Animal Care and Use Committee (IACUC).

### Cell Culture and Drug Treatment

Mouse keratinocytes were cultured and maintained in E-media with 15% serum and 0.05 mM  $\text{Ca}^{2+}$ . Cells were transfected using Effectene transfection reagent (QIAGEN), and then processed for immunofluorescence as described in the Supplemental Experimental Procedures.

For inhibition of mitotic kinases, cells were shifted to high- $\text{Ca}^{2+}$  E-media with the following inhibitors for 3–8 hr (cultured cells) or 4 hr (explants): for Plk1, BI2536 (Selleck Chemicals, 300 nM); and for AuroraA/B, VX-680 (Selleck Chemicals, 700 nM). For transferrin internalization, 3  $\mu\text{g}/\text{ml}$  transferrin-Alexa546 was added to cells that had been treated with 300 nM BI2536 or DMSO for 2 hr. After 30 min incubation at 37 degrees, cells were washed three times in cold PBS and fixed with 4% paraformaldehyde.

### Antibodies

Primary antibodies were used at the following dilutions: GFP (chicken, Abcam), 1:2,000;  $\beta$ -tubulin (mouse, Sigma), 1:500; Flag (mouse, Stratagene), 1:2,000; Celsr1 (guinea pig, Devenport and Fuchs, 2008), 1:500; E-cadherin (rat, Thermo Pierce), 1:1,000; and phospho-histone H3-Ser10 (rabbit, Upstate), 1:1,000. The phospho-specific antibody against Celsr1 pT2750 was custom-generated by 21<sup>st</sup> Century Biochemicals (Marlboro, MA) by immunizing rabbits with the peptide ATTRATLL[pT]RSLN. Serum was affinity purified to ensure phosphospecificity and used at 1:1,000.

### Imaging

Confocal images were acquired with an inverted A1 or A1R-Si on a Nikon Eclipse Ti (Nikon Instruments) equipped with GaASP detectors and a 60 $\times$  oil objective (numerical aperture, NA 1.4) using NIS-Elements software (Nikon). Images shown are maximum projections of z stacks, created and processed using NIS-elements. TIRF images were acquired on a Nikon TIRF illuminator on Ti-E (Nikon) with a 60 $\times$  oil objective (NA 1.49) and an iXon Ultra (Andor) camera using NIS-Elements. Green and red channels were acquired sequentially every 20–100 ms for 5–10 min. Live imaging was performed on a Ti-E (Nikon) with a Yokogawa spinning disc (CSU-21) with a 60 $\times$  oil objective (NA 1.4), equipped with Hamamatsu ImageM back thinned EMCCD detector, using NIS-Elements. The z stacks (15 slices, 0.3  $\mu\text{m}$ ) were collected at every 2 min for 45–90 min, or until the cell completed mitosis.

### Image Analysis and Quantification

Quantification of mitotic internalization was performed by calculating M1 coefficients representing the colocalization of Celsr1/E-Celsr1CT puncta per cell, using ImageJ plugin JaCoP. Celsr1 asymmetry in BI2536-treated explants was quantified using ImageJ by calculating Celsr1 mean intensities at their corresponding pixel angles relative to the cell centroid. Pixel angles were plotted against intensities in a rose diagram using MATLAB.

Celsr1 asymmetry in cells bordering mitotic cells in BI2536-treated explants was calculated using Packing Analyzer V2 (Aigouy et al., 2010) and as further described in the Supplemental Experimental Procedures.

### Mass Spectrometry

Celsr1 $\Delta$ N-GFP was immunoprecipitated from keratinocytes using anti-GFP antibodies as described in the [Supplemental Experimental Procedures](#). Liquid chromatography-tandem mass spectrometry (LC-MS/MS) analyses were performed on a high-resolution, high-mass-accuracy, reversed-phase nano-UPLC-MS platform, consisting of an Easy nLC Ultra 1,000 nano-UPLC system coupled to an Orbi Elite mass spectrometer (ThermoFisher Scientific) equipped with a Flex Ion source (Proxeon Biosystems, Odense, Denmark). Analysis was performed as described in the [Supplemental Experimental Procedures](#).

### Plk1 In Vitro Kinase Reaction

1  $\mu$ g of substrate (GST only or GST-tagged Celsr1CT) was incubated with 100 ng of His-tagged Plk1 in kinase buffer (20 mM HEPES, 70 mM NaCl, 5 mM MgCl<sub>2</sub>, 4 mM DTT, 10% glycerol, and 3  $\mu$ Ci  $\gamma$ -<sup>32</sup>P-ATP) in 10  $\mu$ l total volume at 30°C for 30 min. The reaction was stopped by the addition of sample buffer and proteins were separated on a 7.5% SDS gel. The incorporation of  $\gamma$ -<sup>32</sup>P-ATP was visualized by phosphorimaging on a Typhoon FLA-7000 (GE Healthcare).

For details on constructs and methods, see the [Supplemental Experimental Procedures](#).

### SUPPLEMENTAL INFORMATION

Supplemental Information includes Supplemental Experimental Procedures, five figures, five tables, and four movies and can be found with this article online at <http://dx.doi.org/10.1016/j.devcel.2015.03.024>.

### AUTHOR CONTRIBUTIONS

R.S. and D.D. designed the experiments, analyzed and interpreted the data, and wrote the manuscript. R.S. conducted the majority of experiments and image acquisition. D.D. performed TIRF imaging. K.A.L. carried out molecular cloning. J.V.T. performed Celsr1 coimmunoprecipitations for mass spectrometry, W.L. conducted in vitro mitotic kinase inhibition experiments, and D.H.P. provided consultation and analysis of MS experiments.

### ACKNOWLEDGMENTS

We thank Kyung S. Lee for the Plk1-GFP constructs, Henry Shwe for MS data acquisition, Alexei Korennykh and lab members for generous assistance with in vitro kinase assays, and Gary Laevsky for technical assistance with imaging. We are grateful to Rebecca Burdine and Paul Schedl for helpful discussions and to D.D. lab members for discussions and feedback, especially Bryan Heck and Wen Yih Aw for help with image quantification. Work was supported by NIH/NIAMS Pathway to Independence Award R00AR057501.

Received: August 22, 2014

Revised: February 9, 2015

Accepted: March 29, 2015

Published: May 21, 2015

### REFERENCES

Aigouy, B., Farhadifar, R., Staple, D.B., Sagner, A., Röper, J.C., Jülicher, F., and Eaton, S. (2010). Cell flow reorients the axis of planar polarity in the wing epithelium of *Drosophila*. *Cell* **142**, 773–786.

Axelrod, J.D. (2001). Unipolar membrane association of Dishevelled mediates Frizzled planar cell polarity signaling. *Genes Dev.* **15**, 1182–1187.

Barr, F.A., Silljé, H.H., and Nigg, E.A. (2004). Polo-like kinases and the orchestration of cell division. *Nat. Rev. Mol. Cell Biol.* **5**, 429–440.

Bastock, R., Strutt, H., and Strutt, D. (2003). Strabismus is asymmetrically localized and binds to Prickle and Dishevelled during *Drosophila* planar polarity patterning. *Development* **130**, 3007–3014.

Chen, W.S., Antic, D., Matis, M., Logan, C.Y., Povelones, M., Anderson, G.A., Nusse, R., and Axelrod, J.D. (2008). Asymmetric homotypic interactions of the

atypical cadherin flamingo mediate intercellular polarity signaling. *Cell* **133**, 1093–1105.

Devenport, D., and Fuchs, E. (2008). Planar polarization in embryonic epidermis orchestrates global asymmetric morphogenesis of hair follicles. *Nat. Cell Biol.* **10**, 1257–1268.

Devenport, D., Oristian, D., Heller, E., and Fuchs, E. (2011). Mitotic internalization of planar cell polarity proteins preserves tissue polarity. *Nat. Cell Biol.* **13**, 893–902.

Elia, A.E., Cantley, L.C., and Yaffe, M.B. (2003a). Proteomic screen finds pSer/pThr-binding domain localizing Plk1 to mitotic substrates. *Science* **299**, 1228–1231.

Elia, A.E., Rellos, P., Haire, L.F., Chao, J.W., Ivins, F.J., Hoepker, K., Mohammad, D., Cantley, L.C., Smerdon, S.J., and Yaffe, M.B. (2003b). The molecular basis for phosphodependent substrate targeting and regulation of Plks by the Polo-box domain. *Cell* **115**, 83–95.

Fernández-Miñán, A., Martín-Bermudo, M.D., and González-Reyes, A. (2007). Integrin signaling regulates spindle orientation in *Drosophila* to preserve the follicular-epithelium monolayer. *Curr. Biol.* **17**, 683–688.

Goodrich, L.V., and Strutt, D. (2011). Principles of planar polarity in animal development. *Development* **138**, 1877–1892.

Guo, N., Hawkins, C., and Nathans, J. (2004). Frizzled6 controls hair patterning in mice. *Proc. Natl. Acad. Sci. USA* **101**, 9277–9281.

Hao, Y., Du, Q., Chen, X., Zheng, Z., Balsbaugh, J.L., Maitra, S., Shabanowitz, J., Hunt, D.F., and Macara, I.G. (2010). Par3 controls epithelial spindle orientation by aPKC-mediated phosphorylation of apical Pins. *Curr. Biol.* **20**, 1809–1818.

Jaffe, A.B., Kaji, N., Durgan, J., and Hall, A. (2008). Cdc42 controls spindle orientation to position the apical surface during epithelial morphogenesis. *J. Cell Biol.* **183**, 625–633.

Kettenbach, A.N., Schweppe, D.K., Faherty, B.K., Pechenick, D., Pletnev, A.A., and Gerber, S.A. (2011). Quantitative phosphoproteomics identifies substrates and functional modules of Aurora and Polo-like kinase activities in mitotic cells. *Sci. Signal.* **4**, rs5.

Lawrence, P.A., Casal, J., and Struhl, G. (2004). Cell interactions and planar polarity in the abdominal epidermis of *Drosophila*. *Development* **131**, 4651–4664.

Lee, K.S., Park, J.E., Kang, Y.H., Zimmerman, W., Soung, N.K., Seong, Y.S., Kwak, S.J., and Erikson, R.L. (2008). Mechanisms of mammalian polo-like kinase 1 (Plk1) localization: self- versus non-self-priming. *Cell Cycle* **7**, 141–145.

Lénárt, P., Petronczki, M., Steegmaier, M., Di Fiore, B., Lipp, J.J., Hoffmann, M., Rettig, W.J., Kraut, N., and Peters, J.M. (2007). The small-molecule inhibitor BI 2536 reveals novel insights into mitotic roles of polo-like kinase 1. *Curr. Biol.* **17**, 304–315.

Lowery, D.M., Clauser, K.R., Hjerrild, M., Lim, D., Alexander, J., Kishi, K., Ong, S.E., Gammeltoft, S., Carr, S.A., and Yaffe, M.B. (2007). Proteomic screen defines the Polo-box domain interactome and identifies Rock2 as a Plk1 substrate. *EMBO J.* **26**, 2262–2273.

Martin-Belmonte, F., and Perez-Moreno, M. (2012). Epithelial cell polarity, stem cells and cancer. *Nat. Rev. Cancer* **12**, 23–38.

Nakajima, H., Toyoshima-Morimoto, F., Taniguchi, E., and Nishida, E. (2003). Identification of a consensus motif for Plk (Polo-like kinase) phosphorylation reveals Myt1 as a Plk1 substrate. *J. Biol. Chem.* **278**, 25277–25280.

Neef, R., Gruneberg, U., Kopajtich, R., Li, X., Nigg, E.A., Silljé, H., and Barr, F.A. (2007). Choice of Plk1 docking partners during mitosis and cytokinesis is controlled by the activation state of Cdk1. *Nat. Cell Biol.* **9**, 436–444.

Nigg, E.A. (2001). Mitotic kinases as regulators of cell division and its checkpoints. *Nat. Rev. Mol. Cell Biol.* **2**, 21–32.

Oppermann, F.S., Grundner-Culemann, K., Kumar, C., Gruss, O.J., Jallepalli, P.V., and Daub, H. (2012). Combination of chemical genetics and phosphoproteomics for kinase signaling analysis enables confident identification of cellular downstream targets. *Mol. Cell. Proteomics* **11**, O111.012351.

Park, J.E., Soung, N.K., Johmura, Y., Kang, Y.H., Liao, C., Lee, K.H., Park, C.H., Nicklaus, M.C., and Lee, K.S. (2010). Polo-box domain: a versatile mediator of polo-like kinase function. *Cell. Mol. Life Sci.* **67**, 1957–1970.

- Ravni, A., Qu, Y., Goffinet, A.M., and Tissir, F. (2009). Planar cell polarity cadherin *Celsr1* regulates skin hair patterning in the mouse. *J. Invest. Dermatol.* *129*, 2507–2509.
- Reinsch, S., and Karsenti, E. (1994). Orientation of spindle axis and distribution of plasma membrane proteins during cell division in polarized MDCKII cells. *J. Cell Biol.* *126*, 1509–1526.
- Roignot, J., Peng, X., and Mostov, K. (2013). Polarity in mammalian epithelial morphogenesis. *Cold Spring Harb. Perspect. Biol.* *5*, 5.
- Santamaria, A., Wang, B., Elowe, S., Malik, R., Zhang, F., Bauer, M., Schmidt, A., Sillje, H.H., Korner, R., and Nigg, E.A. (2011). The Plk1-dependent phosphoproteome of the early mitotic spindle. *Mol. Cell. Proteomics* *10*, M110.004457.
- Simons, M., and Mlodzik, M. (2008). Planar cell polarity signaling: from fly development to human disease. *Annu. Rev. Genet.* *42*, 517–540.
- Stegmaier, M., Hoffmann, M., Baum, A., Lénárt, P., Petronczki, M., Krssák, M., Gürtler, U., Garin-Chesa, P., Lieb, S., Quant, J., et al. (2007). BI 2536, a potent and selective inhibitor of polo-like kinase 1, inhibits tumor growth in vivo. *Curr. Biol.* *17*, 316–322.
- Struhl, G., Casal, J., and Lawrence, P.A. (2012). Dissecting the molecular bridges that mediate the function of Frizzled in planar cell polarity. *Development* *139*, 3665–3674.
- Strutt, D.I. (2001). Asymmetric localization of frizzled and the establishment of cell polarity in the *Drosophila* wing. *Mol. Cell* *7*, 367–375.
- Strutt, H., and Strutt, D. (2009). Asymmetric localisation of planar polarity proteins: mechanisms and consequences. *Semin. Cell Dev. Biol.* *20*, 957–963.
- Taylor, J., Abramova, N., Charlton, J., and Adler, P.N. (1998). Van Gogh: a new *Drosophila* tissue polarity gene. *Genetics* *150*, 199–210.
- Traub, L.M., and Bonifacino, J.S. (2013). Cargo recognition in clathrin-mediated endocytosis. *Cold Spring Harb. Perspect. Biol.* *5*, a016790.
- Tree, D.R., Shulman, J.M., Rousset, R., Scott, M.P., Gubb, D., and Axelrod, J.D. (2002). Prickle mediates feedback amplification to generate asymmetric planar cell polarity signaling. *Cell* *109*, 371–381.
- Usui, T., Shima, Y., Shimada, Y., Hirano, S., Burgess, R.W., Schwarz, T.L., Takeichi, M., and Uemura, T. (1999). Flamingo, a seven-pass transmembrane cadherin, regulates planar cell polarity under the control of Frizzled. *Cell* *98*, 585–595.
- Vinson, C.R., and Adler, P.N. (1987). Directional non-cell autonomy and the transmission of polarity information by the frizzled gene of *Drosophila*. *Nature* *329*, 549–551.
- Vladar, E.K., Antic, D., and Axelrod, J.D. (2009). Planar cell polarity signaling: the developing cell's compass. *Cold Spring Harb. Perspect. Biol.* *1*, a002964.
- Wurzenberger, C., and Gerlich, D.W. (2011). Phosphatases: providing safe passage through mitotic exit. *Nat. Rev. Mol. Cell Biol.* *12*, 469–482.